

Critical phases in the raise and peel model

D. A. C. Jara^{1,2}, and F. C. Alcaraz¹

¹ *Instituto de Física de São Carlos, Universidade de São Paulo, Caixa Postal 369,
13560-590, São Carlos, SP, Brazil*

² *Facultad de Ingenieria, Universidad de La Sabana, A.A. 53753, Chia, Colombia*

October 10, 2018

Abstract

The raise and peel model (RPM) is a nonlocal stochastic model describing the space and time fluctuations of an evolving one dimensional interface. Its relevant parameter u is the ratio between the rates of local adsorption and nonlocal desorption processes (avalanches) processes. The model at $u = 1$ give us the first example of a conformally invariant stochastic model. For small values $u < u_0$ the model is known to be non-critical, while for $u > u_0$ it is critical. Although previous studies indicate that $u_0 = 1$ the determination of u_0 with a reasonable precision is still missing. By calculating the structure function of the height profiles in the reciprocal space we confirm with good precision that indeed $u_0 = 1$. We establish that at the conformal invariant point $u = 1$ the RPM has a roughness transition with dynamical and roughness critical exponents $z = 1$ and $\alpha = 0$, respectively. For $u > 1$ the model is critical with an u -dependent dynamical critical exponent $z(u)$ that tends towards zero as $u \rightarrow \infty$. However at $1/u = 0$ the RPM is exactly mapped into the totally asymmetric exclusion problem (TASEP). This last model is known to be noncritical (critical) for open (periodic) boundary conditions. Our studies indicate that the RPM as $u \rightarrow \infty$, due to its nonlocal dynamics processes, has the same large-distance physics no matter what boundary condition we chose. For $u > 1$, our analysis show that differently from previous predictions, the region is composed by two distinct critical phases. For $u \leq u < u_c \approx 40$ the height profiles are rough ($\alpha = \alpha(u) > 0$), and for $u > u_c$ the height profiles are flat at large distances ($\alpha = \alpha(u) < 0$). We also observed that in both critical phases ($u > 1$) the RPM at short length scales, has an effective behavior in the Kardar-Parisi-Zhang (KPZ) critical universality class, that is not the true behavior of the system at large length scales.

¹dacj1984@gmail.com

²alcaraz@if.sc.usp.br

1 Introduction

The raise and peel model (RPM) on its original formulation [1, 2, 3] is a stochastic model describing the time and space fluctuations of restricted solid-on-solid (RSOS) one dimensional profiles. They define an interface separating a solid phase from a rarefied gas of tiles, and change as the tiles coming from the rarefied gas phase reach the interface. The tiles can be locally absorbed (raise) or can trigger a nonlocal desorption of tiles (peel) in the surface of the solid phase. The model is defined in terms of a free parameter u given by the ratio between the adsorption and desorption rates. The RSOS fluctuating profiles can also represent the configurations of excluded volume particles in a discrete lattice. The RPM in this case [4] gives a generalization of the asymmetric exclusion problem (ASEP) [5], where the excluded volume particles are allowed to have local jumps to the sites on the left and nonlocal ones to the sites on the right. The parameter u defines the anisotropy left/right of the possible motions.

The model at $u = 1$ (equal rates of adsorption and desorption) is special. Its time-evolution operator (Hamiltonian) is exactly integrable and give us the first example of a stochastic model conformally invariant. Its Hamiltonian is given in terms of the generators of the Temperley-Lieb algebra. The model, for the case of open boundaries, can be mapped onto the spin-zero sector of the XXZ quantum chain with the quantum $U_q(Sl(2))$ symmetry with $q = e^{i\frac{\pi}{3}}$ [1, 2, 3]. In the case of periodic boundaries it is related to a XXZ quantum chain with twisted boundary condition [4] (twisted angle $\phi = \frac{2\pi}{3}$).

For $u \neq 1$ all the known results of the RPM comes from numerical analysis. In the original presentation of the model [1] it was not clear if a phase transition exists for $u = u_0 \approx 0.5$ separating a massive phase ($u < u_0$) from a critical phase ($u > u_0$). The value $u_0 \approx 0.5$ was suggested from the mass-gap amplitude crossings of the eigenenergies of the associated Hamiltonian, with open (free) boundary conditions. In [2] numerical studies, based on Monte Carlo simulations, also with the RPM with open boundaries, indicate that $u_0 = 1$. Moreover for $u > 1$ the model is in a self-organized criticality (SOC) phase where the dynamical critical exponent decreases from the value $z = 1$, at the conformal invariant point $u = 1$, to the value $z = 0$ when $u \rightarrow \infty$ (no desorption).

In this paper we present an extensive numerical study of the phase diagram of the RPM. The original motivation of these calculations is due to the exact connection [6] of the RPM with no desorption ($1/u = 0$) with the totally asymmetric exclusion problem (TASEP) [7, 8]. The TASEP is critical ($z = 3/2$) or not depending if the boundary condition is periodic or not. Since all the previous calculations of the dynamical critical exponents were done only in the case of open boundaries is it important to verify if indeed the critical behavior (critical exponents) are the same for both boundaries, differently of the limiting case $1/u = 0$. Measuring several distinct observables we were able to confirm that indeed the massive phase ends up at the critical point $u = u_0 = 1$. By calculating the roughness of the profiles we then verified that the RPM has a roughness transition at $u = 1$, with roughness critical exponent $\alpha = 0$.

for $u > 1$ we obtain some unexpected results that were not observed in the previous calculations of the RPM with open ends [2, 3]. Differently from previous studies, where it was expected a single critical phase, our results indicate the existence of two distinct critical

phases: $1 \leq u \leq u_c$ and $u > u_c$, with $u_c \approx 40$. The intermediate phase ($1 \leq u \leq u_c$) is rough with a roughness critical exponent $\alpha = \alpha(u) \geq 0$. The second phase ($u > u_c$) is critical and flat at large length scales. In this last phase the average height, as the lattice size increases, reaches a limit in the case of open boundaries. In the periodic case the average height of the surface increases with time, reaching a stationary finite velocity. This velocity corresponds to a limiting current in the particle formulation of the RPM [4].

We also verified that the time-evolution in both critical phases exhibits the phenomena of *critical initial slip* [10]. A phenomena that induces the appearance, for a quite large time interval, of an effective exponent that depends on the particular configuration where the system starts its evolution. This phenomena produces difficulties in the evaluation of the dynamical critical exponent by using the Family-Vissek scaling, as reported in earlier calculations of the RPM [2]. To avoid this effect we should calculate observables directly in the stationary state. A quite reasonable assumption of the scaling behavior of the height profiles at the stationary regime indicates a possible way to evaluate the dynamical critical exponent.

Our results indicate that independently of the boundary condition, as $u \rightarrow \infty$, the dynamical critical exponent goes to zero. This is distinct from the case where we set $1/u = 0$ (no desorption). In this limiting case we recover the TASEP, a stochastic model that is critical and belongs to the Kardar-Parisi-Zhang (KPZ) universality class [9], only if the boundary conditions are closed (periodic). In order to see how the height profiles change as we approach the limiting case $u = u_0 = 1$ and $u \rightarrow \infty$ we calculate the spatial structure function of the height profiles. The results show us clearly crossover effects to the KPZ behavior as u increases, and allow us to understand the distinct behavior in both critical phases.

The paper is organized as follows. In the next section, in order to set the notations we present the RPM as well the observables that will be considered along the paper. In section 3 we give the results that confirm that for $u < u_0$ the model is noncritical, being $u_0 = 1$ (conformally invariant point) the critical point, where the model is conformally invariant. The section 4 is devoted to the evaluation of the critical exponents for $u > u_0 = 1$, by using several distinct methods. In section 5 we calculate the spatial structure function of the height profiles. The results indicate the existence of two distinct critical phases. Finally in section 6 we present our concluding remarks.

2 Description of the raise and peel model

The stochastic model RPM has a free parameter u and is already described in several papers [1, 2, 3]. The model, for the special value $u = 1$, gives the first example of a conformally invariant stochastic model (central charge $c = 0$). Its time-evolution operator (Hamiltonian) is related to the exact integrable XXZ quantum chain with anisotropy $\Delta = -1/2$ and special boundaries [1, 2, 3]. At this conformal invariant point the model is also interesting, from the mathematical point of view since, as observed by Razumov and Stroganov [12], the probability distribution of the system's configurations is related to the interesting problem of enumerating alternated sign matrices.

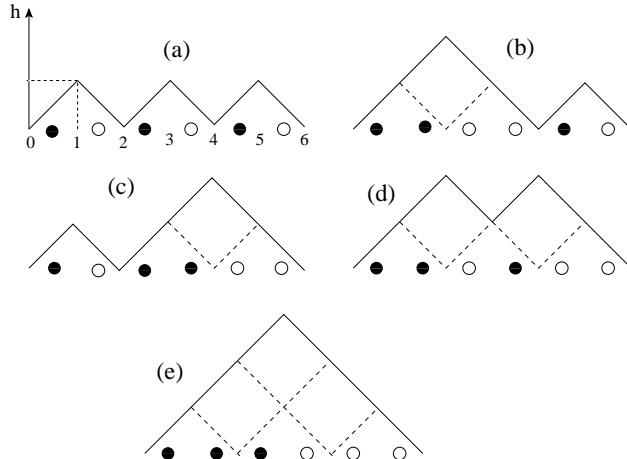


Figure 1: The five configurations of the RPM for a lattice with $L = 6$ sites and open boundary conditions. The configurations in the particle-vacancy representation are also shown: particles and vacancies are denoted by full and empty circles.

We are going to describe the model in two distinct, but equivalent, stochastic bases (configuration's space). The first one, that we named the height representation basis, is given in terms of Dyck paths. These paths are defined in terms of integer heights $\{h_i\}$ obeying the restricted solid-on-solid (SOS) rules:

$$h_{i+1} - h_i = \pm 1. \quad (2.1)$$

For open systems $i = 0, 1, 2, \dots, L$ and $h_0 = h_L = 0$, and for the periodic ones $i = 1, 2, \dots, L$ and $h_i = h_{i+L}$. We consider in this paper L as an even number. There are $L!/\{(L+2)([L/2]!)^2\}$ configurations for the open systems and $L!/([L/2]!)^2$ for the periodic case. The second basis, we formulated the RPM, is the one we call particle-vacancy basis [4]. It is given by the configurations of $L/2$ excluded volume particles and $L/2$ vacancies. The configurations in this last basis are obtained from the height representation one by inserting particles or vacancies at the links $(i, i+1)$, depending if $h_{i+1} > h_i$ or $h_{i+1} < h_i$, respectively. In Figs. 1 and 2 we show the configurations in both basis for the $L = 6$ model with open boundaries and for the $L = 4$ model with periodic boundaries, respectively.

In the height basis we can visualize the stochastic evolution of the RPM by considering the profiles $\{h_i\}$ as an one dimensional surface separating a solid from a rarefied gas phase of tilted tiles (see Fig. 3). The profiles changes due to the hits of tiles coming from the rarefied gas phase, according to the following rules:

During a short time interval Δt at most one tile from the gaseous phase reaches the surface. With a probability $p = \Delta t/L$ a tile reaches the site i of the surface (see Fig. 3). The allowed motions depend on the local heights (h_{i-1}, h_i, h_{i+1}) .

i) If $h_{i-1} < h_i > h_{i+1}$ the tile reaches a local peak (case (b) of Fig. 3). The tile is reflected with no changes in the surface profile.

ii) If $h_{i-1} > h_i < h_{i+1}$ the tile reaches a local minimum (case (d) of Fig. 3). With a probability p_a , proportional to the absorption rate W_a , the tile is added to the surface

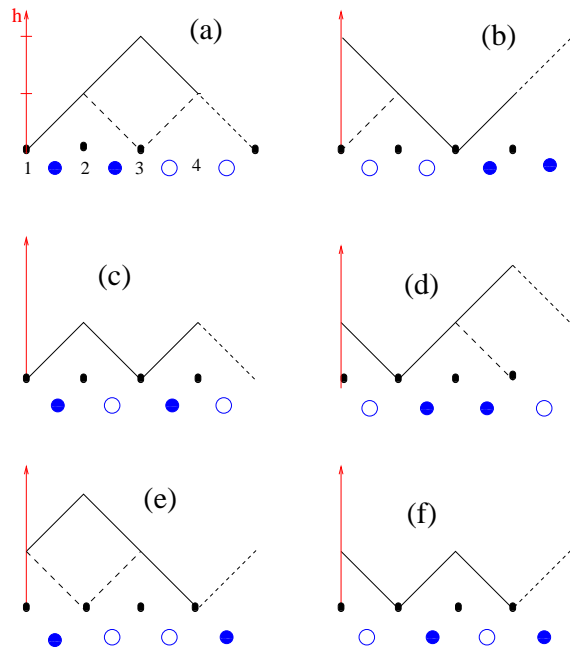


Figure 2: The 6 possible profiles for the RPM with periodic boundaries and $L = 4$ sites. The configurations in the particle-vacancy representation are also shown: particles and vacancies are denoted by full and empty circles.

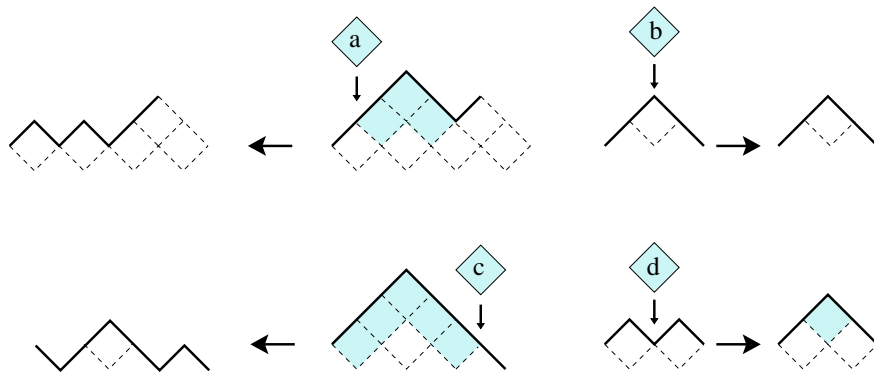


Figure 3: The dynamical processes in the RPM. The tilted tile in the gaseous phase hit a positive slope (a), a peak in (b), a negative slope in (c) and a valley in (d) (see the text).

($h_i \rightarrow h_i + 2$) and with a probability $1 - p_a$ the tile is reflected, with no change in the surface profile.

iii) If $h_{i-1} < h_i < h_{i+1}$ the tile reaches a positive slope (case (a) of Fig. 3). With a probability p_d proportional to the desorption rate W_d , the tile is reflected after desorbing ($h_i \rightarrow h_i - 2$) a layer of $(b - 1)$ tiles from the segment $\{h_j\}$ ($j = i + 1, \dots, i + b - 1$), where $h_j > h_i = h_{i+b}$. With the probability $1 - p_d$ the tile is reflected and no changes happen in the surface.

iv) If $h_{i-1} > h_i > h_{i+1}$ the tile reaches a negative slope (case (c) of Fig. 3). With a probability p_d , proportional to the desorption rate W_d , the tile is reflected after desorbing ($h_j \rightarrow h_j - 2$) a layer of $(b - 1)$ tiles from the segment $\{h_j\}$ ($j = i - b + 1, \dots, i - 1$), where $h_j > h_i = h_{i-b}$. With a probability $1 - p_d$ the tile is reflected and the surface is unchanged.

The relevant parameter in the dynamics of the RPM is the ratio among the adsorbing and desorbing rates $u = W_a/W_d$. In a continuous time evolution the time fluctuations of the probabilities $P_c(t)$ of finding the system in a configuration c is given by the master equation

$$\frac{dP_c(t)}{dt} = \sum_{c'} H_{c,c'} P_{c'}(t), \quad (2.2)$$

where $H_{c,c'}$ are the matrix elements of the Hamiltonian governing the stochastic evolution. As an example, the Hamiltonian H for the open chain with $L = 6$ sites, connecting the five configurations of Fig. 1, is given by

$$H = - \begin{pmatrix} & \langle a | & \langle b | & \langle c | & \langle d | & \langle e | \\ \langle a | & -2u & 2 & 2 & 0 & 2 \\ \langle b | & u & -(u+2) & 0 & 1 & 0 \\ \langle c | & u & 0 & -(u+2) & 1 & 0 \\ \langle d | & 0 & u & u & -(u+2) & 2 \\ \langle e | & 0 & 0 & 0 & u & -4 \end{pmatrix}, \quad (2.3)$$

where we take $u_d = 1$ and $u = u_a$.

The dynamic rules for the RPM, in the particle-vacancy basis, follows from the correspondence of the configurations in this basis with those in the height basis. In this representation the particles (only the particles) can make jumps to the leftmost position with probability proportional to W_a , provide it is empty (has a vacancy), or may do a nonlocal jump to empty positions on its right, leaving a segment with equal number of particles and vacancies. The probability of these jumps to the right are proportional to the desorption rate and depends also on the configuration of the particles. In Fig. 4 we give schematically the allowed motions of particles in the particle-vacancy basis (see also [4]).

Due to the dynamics of the RPM in the case of open boundaries two configurations have special importance: the *substrate* and the *pyramid* configurations. The substrate configuration is the one where $h_i = h_{i+2}$ ($i = 0, 1, \dots, L$) and no desorptions are allowed. In Fig. 1 it is the configuration (a). The pyramid configuration is the one where $h_i = i$ ($i = 0, \dots, L/2$) and $h_i = L - i$ ($i = \frac{L}{2} + 1, \dots, L$), and only desorptions may take place. In Fig. 1 is the configuration (e).

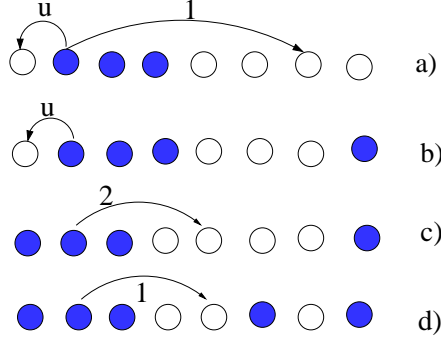


Figure 4: a,b) Hopping rules if the particle is preceded by a vacancy. c,d) Hopping rules if the particle is preceded by another particle.

In the following sections, in order to characterize the phase diagram of the RPM, we are going to evaluate some observables. An important one is the average height of the profile at time t :

$$h(L, t) = \frac{1}{L} \sum_{i=1}^L \langle h_i(t) \rangle, \quad (2.4)$$

where $\langle h_i(t) \rangle$ is the average height at site $i = 1, \dots, L$ in the height representation. The Fourier transform of the heights

$$h(k, t) = \frac{1}{L^{1/2}} \sum_{j=1}^L (h_j(t) - h(L, t)) \exp(ikj), \quad (2.5)$$

give us the structure function

$$S(k, t) = \langle h(k, t) h(-k, t) \rangle, \quad k = \frac{2\pi j}{L} \quad (j = -L/2, \dots, L/2), \quad (2.6)$$

that reveals the structure of the height profiles at the spatial length $\lambda = 2\pi/k$.

In the open boundary case it is interesting to define the contact points and the clusters. Contact points are the sites of a given profile where the height is zero and the profile makes a contact with the substrate at $h = 0$, as for example the points 0, 4 and 6 of the configurations (b) of Fig. 1. The heights between two consecutive contact points, with tiles added in the substrate is defined as a cluster. In Fig. 1 there are one cluster in configurations ((b), (c), (d) and (e), and no cluster in the substrate configuration (a).

3 The phase transition at $u = u_0 = 1$

For $u \ll 1$ the RPM is clearly in a massive phase. The stationary asymptotic state (ground state of the Hamiltonian) is given basically by a combination of the substrate configuration and the ones obtained from the addition of few tiles in the substrate. We have a combination of a large number of clusters with finite size, independent of the lattice size, for sufficiently large lattice sizes. As u increases the characteristic size of the clusters increases and at $u = u_0$

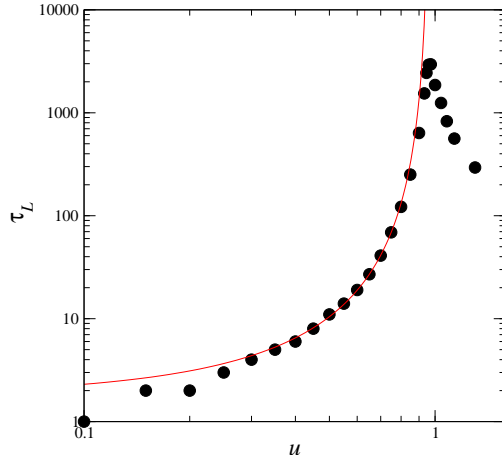


Figure 5: The characteristic time τ_L (units of Monte Carlos steps) necessary to reach the stationary state, as a function of u . The RPM has $L = 16384$ sites, open ends, and the initial configuration is the substrate one.

it diverges with the lattice size. The precise determination of the critical point $u = u_0$, where the massive phase ends, is not simple.

In [1], where the RPM was introduced, numerical calculations of the mass gap crossings of the Hamiltonian with small lattice sizes and open boundary conditions indicates that $u_0 \approx 0.5$. However the finite-size effects around $u \approx u_0$ are quite large. To illustrate them we show in Fig. 5 the characteristic time τ_L , as a function of u , necessary for the system to reach the stationary state, by starting ($t = 0$) with the substrate configuration of a lattice with $L = 2^{14} = 16384$ sites. The fitting curve, shown in red in Fig. 5 indicates $\tau_L \sim (u_0 - u)^{-\nu_t}$, with $u_0 = 0.96$ and $\nu_t = 2.43$. Although the lattice size is relatively large, by increasing the lattice size for $L > 2^{17} = 131072$ we verified that the predicted value of u_0 increases. In fact a previous calculation [2], based on the density of clusters, although considering a relatively small lattice size ($L = 2^{16} = 65636$) indicates that $u_0 = 1$.

Although we have done measurements of several observables for large lattice sizes that confirms the phase transition at $u = u_0 = 1$, we are going to present in this section the measurements of only two of these observables, with the lattice taken with free boundaries. The first one is the average size of a cluster CS , that we define as:

$$CS = \sum_{k=1}^{N_c} s_k \left(\frac{s_k}{N_{oc}} \right), \quad (3.1)$$

where s_k is the number of tiles in the first row ($h = 2$) of the k th cluster ($k = 1, 2, \dots, N_c$), N_c is the number of clusters and $N_{oc} = \sum_{k=1}^{N_c} s_k$ is the total number of tiles in the first row of the profile configuration. The quantity CS can be interpreted as follows. If we chose a random site among the ones having tiles in the first row ($h_i \geq 2$), CS gives the average size of the cluster where the chosen site belongs.

In Figs. 6a and 6b we show CS for lattice sizes up to $L = 2^{19} = 524, 288$ for $u = 0.98$ and $u = 1$, respectively. We clearly see in Fig. 6a that for $u = 0.98$ the lattice sizes $L > 100000$ indicate a saturation value for a finite cluster size as $L \rightarrow \infty$, as we should expect in a

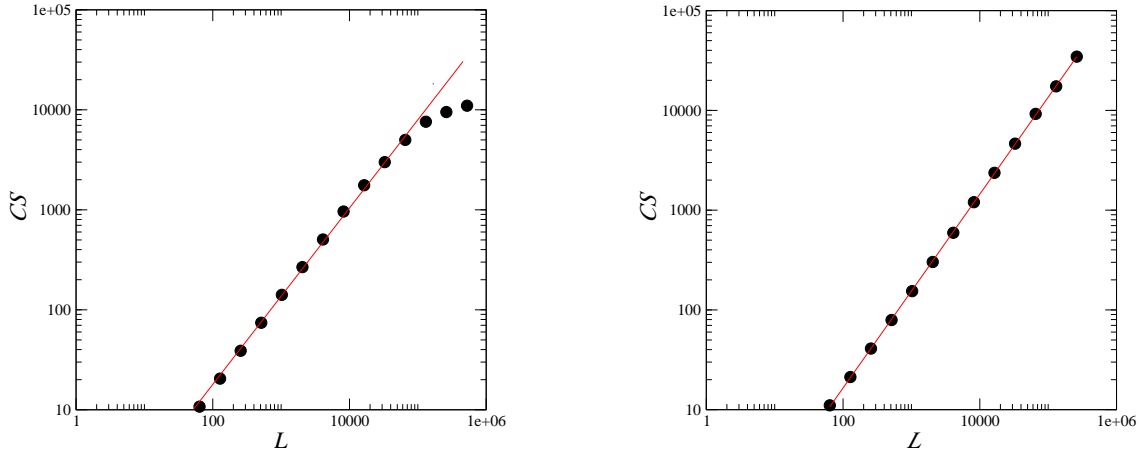


Figure 6: Average cluster size CS (black dots), in the stationary state of the RPM with open boundaries, as a function of the lattice size L . a) $u = 0.98$, b) $u=1$. The red lines are guides to show the deviations from a straight line.

massive phase. On the other hand at $u = 1$, as shown in Fig. 6b, the average cluster size diverges with the lattice size.

The second observable we measured to confirm $u_0 = 1$ is the spatial structure function of the profiles at the stationary state ($t \rightarrow \infty$), defined in (2.5)-(2.6). For several values of u the structure function $S(1/\lambda, t \rightarrow \infty)$, for the lattice size $L = 524, 382$ is shown in Fig. 7. The values of u in the figure are, from right to left, $u = 0.50, 0.55, \dots, 0.90, 0.95$. We see in this figure that at short length scales, i. e., $\lambda \lesssim \lambda_1(u)$ the structure function behaves as $S(\lambda, t \rightarrow \infty) \sim \lambda$ (or $\sqrt{S(\lambda, t \rightarrow \infty)}/\lambda \sim \text{const.}$), while for large scales $\lambda \gtrsim \lambda_1(u)$ it behaves as $S(1/\lambda, t \rightarrow \infty) \sim \text{const.}$, implying that the profiles are composed by finite-size clusters whose typical sizes increases with u . The constant behavior for $\sqrt{S(1/\lambda, t \rightarrow \infty)}/\lambda$ in Fig. 7, for $\lambda < \lambda_1(u)$, i. e., $S(1/\lambda, t \rightarrow \infty) \sim \lambda$, is a consequence of a crossover effect due to the critical behavior at the conformal invariant point $u = 1$, since as we will see in section 5 $S(1/\lambda, t \rightarrow \infty) \sim \lambda$ (see Eq. (5.5)).

Fig. 7 also explains the strong finite-size effects for $u \gtrsim 0.95$, as we saw in Fig. 6a. For the model with $u = 0.95$ we see an "effective critical" crossover effect up to $\lambda \sim 10^5$, implying that the massive behavior of the model can only be seen for lattice sizes $L \gtrsim 10^5$, in agreement with the results shown in Fig. 6a.

In order to get a precise estimate of the critical point u_0 from Fig. 7 we consider the wavelength $\lambda_{\text{small}}(u)$ obtained from the crossing of the two distinct asymptotic behaviors, namely, the one for $\lambda \rightarrow \infty$ and the one expected at $u = 1$ (horizontal line in Fig. i7). Those are the points marked in (*) in Fig. 7. In Fig. 8 we plot $\lambda_{\text{small}}(u)$ and we got the fit

$$1/\lambda_{\text{small}}(u) = a(u - u_0)^b, \quad (3.2)$$

where $a = 0.406(4)$, $u_0 = 1.000(1)$ and the exponent $b = 2.738(7)$, confirming that $u_0 = 1$.

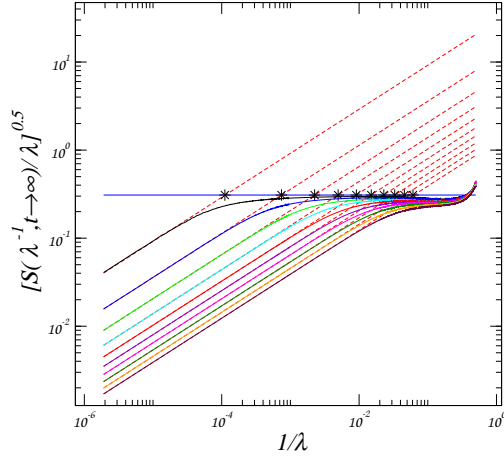


Figure 7: The structure function $S(1/\lambda, t \rightarrow \infty)$ of the RPM at the stationary regime for several values of u and lattice size $L = 524, 382$. The values of u from the top to the bottom are $0.95, 0.90, \dots, 0.55, 0.50$. The red straight lines are obtained by fitting the curves, by considering small values of λ . The straight blue horizontal line is the auxiliary line used to determine the crossing points (*) separating the initial and asymptotic regimes.

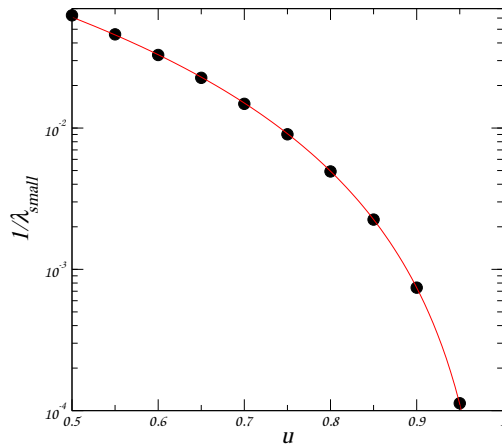


Figure 8: The crossing points $\lambda_{\text{small}}(u)$, represented as (*) in Fig. 7, as a function of u .

4 The critical exponents and phases for $u > 1$

Previous numerical results for the RPM with open [1, 2] and periodic boundary conditions [4] indicate that for $u > 1$ the model is in a critical regime. We are going to present in this section new numerical results that indicate that this critical regime is separated into two critical phases where the profiles exhibit distinct behavior at large scales.

Previous evaluations [2] of the dynamical critical exponent z for $u \geq 1$ indicate a continuous decrease as u increases, tending to $z = 0$ as $u \rightarrow \infty$. On the other hand, more recently [6] it was observed that the RPM at the limiting case $1/u = 0$ recovers exactly the totally asymmetric exclusion problem (TASEP). We can see this correspondence easily from the allowed processes in the particle-vacancy representation of the model. We can see in Fig. 4 that at this limit the particles can only move to the left, provide the leftmost site is empty. All the local and nonlocal jumps to the right are not allowed. The TASEP although critical for periodic chains is not critical for open boundaries. In the periodic critical case it belongs to the Kardar-Parisi-Zhang (KPZ) universality class [9] where the dynamical critical exponent $z = 3/2$ and the roughness critical exponent is $\alpha = 1/2$. A natural question arises for the RPM: is this distinct behavior for different boundaries a characteristic of the $1/u = 0$ limit, or we may have it also in the RPM for u large, but finite? As we shall see our numerical results indicate that these boundary-dependent behaviors only happen at the singular point $1/u = 0$. Once $1/u \neq 0$ the allowed nonlocal jumps, that happen for both boundaries, make the model critical, with a small value for the critical exponent $z(u) \approx 0$, for $1/u \approx 0$, indicating the discontinuity $z(u \rightarrow \infty) - z(1/u = 0) \neq 0$, for the case of periodic boundaries.

A possible way to estimate the dynamical critical exponent $z = z(u)$ of the RPM is obtained from the leading finite-size behavior of the mass gaps associated to the excited eigenvalues E_n ($n = 1, 2, \dots$) of its L -site Hamiltonian (see (2.3) for the case $L = 6$ and open boundaries):

$$E_n = \frac{A_n}{L^z} + o(L^{-z}), \quad n = 1, 2, \dots \quad (4.1)$$

Applying the power method to estimate the lowest eigenstates of the model with free boundaries we were able to calculate the gaps E_1 and E_2 up to $L = 30$. In table 1 we show the estimated values $z(E_1)$ and $z(E_2)$, for some values of u . The values $z(E_1)$ and $z(E_2)$ are obtained from the finite-size extrapolations, where we use in (4.1) the first gap (E_1) and the second gap (E_2), respectively. The differences among $z(E_1)$ and $z(E_2)$ give us an idea of the accuracy of the predictions. For $u \geq 5$ we only calculate $z(E_2)$ due to numerical instabilities.

A possible way to calculate the dynamical critical exponents using lattice sizes $L > 30$ is from the time evolution of some observable. For example taking as observable the average height $h(L, t)$ at time t , we do expect the general time and size dependence:

$$\frac{h(L, t)}{h(L, (\infty))} - 1 = L^{z_2} f(t/L^{z_1}). \quad (4.2)$$

In general, using different initial conditions we may find distinct pairs of the exponents (z_1, z_2) . If we reach an asymptotic regime where we obtain the same exponent z_1 , for any

u	1	1.135	1.5	2	6	10
$z(E_1)$	1.009	0.842	0.731	0.666	-	-
$z(E_2)$	1.009	0.900	0.756	0.642	0.184	0.030

Table 1: Estimated vales of the dynamical critical exponent. The values $z(E_1)$ and $z(E_2)$ are obtained from the extranolation ($L \rightarrow \infty$) (see Eq. (4.1)) where the first and second gap we

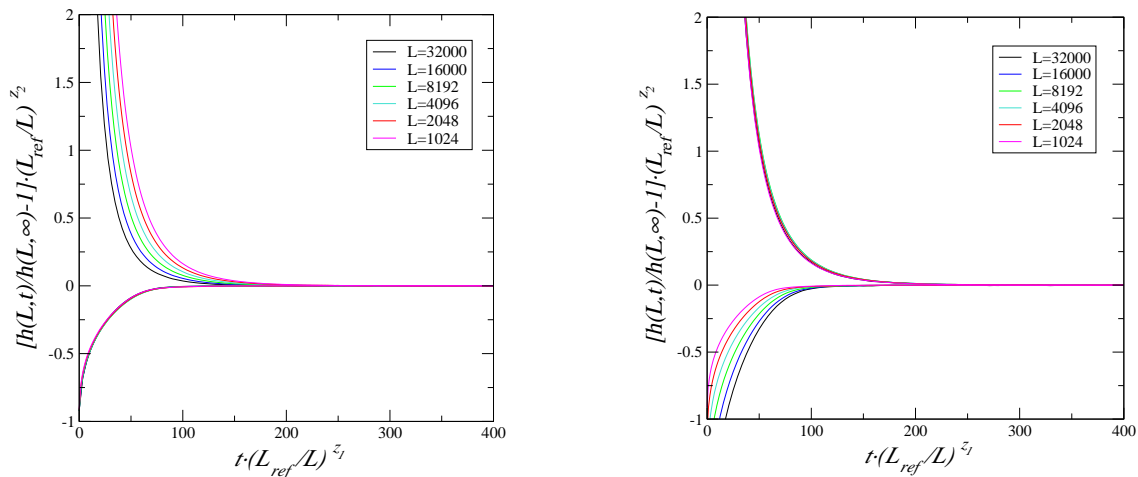


Figure 9: Time evolution curves $(h(L, t)/h(L, \infty) - 1)$, for the RPM with open boundary condition and several lattice sizes. In the top (bottom) curves the initial configuration is the pyramid (substrate). A data collapse of the curves, following Eq. (4.2), is obtained in (a) and (b) by considering as the initial configuration the substrate and the pyramid, respectively. For all the curves the harmless parameter $L_{\text{ref}} = 32000$ is used to better visualize the figures, and 1.610^5 independent runs were averaged.

initial condition, then z_1 is the dynamical critical exponent. If the system is critical and we do not find the same value of z_2 , for distinct initial conditions, we have the effect known as *critical initial slip*, as seen in [10]. In fact for $u > 1$ this effect is present in the RPM, probably due to its nonlocal dynamical processes. In Fig. 9a and 9b we show the time evolution of the average heights (4.2), by taking as the initial configuration the substrate and the pyramid ones, respectively. We obtain a quite good collapse of the curves for the several lattices with $(z_1, z_2) = (0.361, 0.021)$ and $(z_1, z_2) = (0.415, 0.282)$ in Figs. 9a and 9b, respectively. The time interval that would give us the same value of z_1 for both initial conditions happens only at large time and $h(L, t)/h(L, \infty) - 1$ is negligible, preventing a reasonable prediction for z . Other observables, like the number of clusters, also show the same critical initial slip effect.

Due to this memory effect, in order to get a reasonable estimator for the dynamical critical exponent, we should relate this exponent with an observable that can be measured directly at the stationary state. In the case of periodic boundaries this observable does exist. We conjecture that at the stationary regime the average height behaves, apart from a

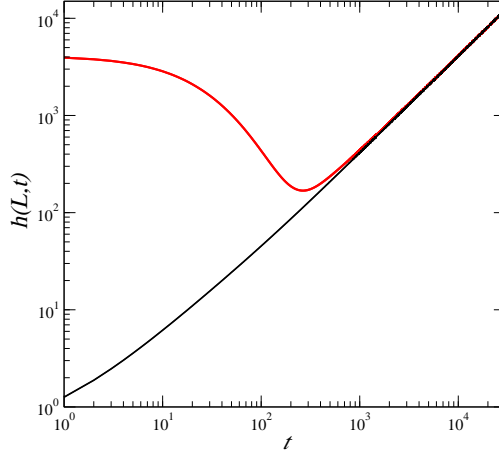


Figure 10: The average height $h(L, t)$ of the RPM with parameter $u = 100$ and periodic boundary conditions. The initial configuration are the substrate (black) and the pyramid (red). The lattice size is $L = 16,384$ and the number of samples in the Monte Carlo simulations is 10,048.

constant, as

$$h_l(t) = L^\alpha f(t/L^z) + v_\infty t, \quad (4.3)$$

where $v_\infty \equiv v(t \rightarrow \infty, L \rightarrow \infty)$ is the bulk limit velocity where the stationary height grows, and α is the roughness critical exponent. The exponent α appears in (4.3) due to the self-affinity of the surface in the stationary state.

The roughness of a profile is defined as [11]

$$\omega(L) = \left[\frac{1}{L} \sum_{j=1}^L (h_j - \bar{h})^2 \right]^{1/2}, \quad (4.4)$$

where $\bar{h} = \sum_{j=1}^L h_j / L$. In a self-affine profile, the exponent α give us the change in the roughness $\omega(L)$ due to a scale dilation ($L \rightarrow bL$): $\omega(bL) = b^\alpha \omega(L)$. In the stationary state the velocity that the surface grows, for a given lattice size L , is given from (4.3) by

$$v(t, L) \equiv \frac{\partial h(L, t)}{\partial t} = \frac{1}{L^{z-\alpha}} g(t/L^z) + v_\infty. \quad (4.5)$$

As an illustration we show in Fig. 10 the time evolution of the average height for the RPM, with $u = 100$, $L = 16384$ and periodic boundaries. The black (red) curve is obtained when the system initiates in the substrate (pyramid) configuration. We see from this figure that $v(t \rightarrow \infty, L)$ coincides for both initial conditions, avoiding thus the critical initial slip effect that appeared in other measures.

It is also interesting to mention that in [14] it was observed that at the roughness transition point ($\alpha = 0$) of a particular model [13], the growth velocity deviates from its maximal value, at $L \rightarrow \infty$, as L^z in agreement with (4.5). Another example happens in the ASEP where the current (related to the velocity in an equivalent growth model) increases as $J_L - J_\infty = a/L$, in agreement with (4.5) since in this case $z = 3/2$ and $\alpha = 1/2$.

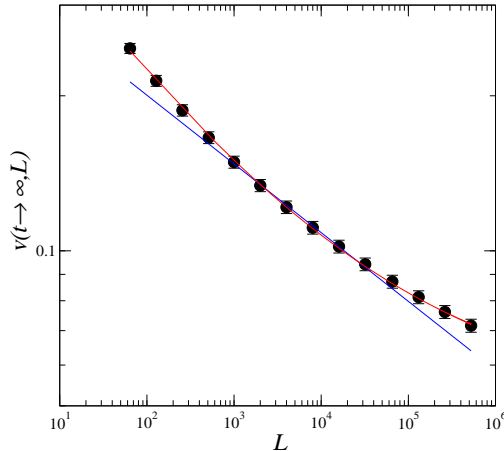


Figure 11: The grow velocity at the stationary regime of the periodic RPM with $u = 5$ and lattice sizes up to $L \sim 500,000$. The blue curve is the linear fit obtained only considering $1,000 \leq L \leq 18,000$.

Previous studies of the RPM with periodic boundaries [4], based on lattice calculations up to lattice size $L \approx 18000$, indicate that the current, in the particle-vacancy representation of the model, or equivalently the growth velocity in the height representation, vanishes for $L \rightarrow \infty$. However the calculations presented in this paper for larger lattices indicate that in fact for $u > 1$ the velocity in the bulk limit is nonzero. As an example we show in Fig. 11 the growth velocity for the model with parameter $u = 5$ and lattice sizes up to $L \sim 500,000$. We also show in the figure the fitted curve (blue) for the lattice sizes $1000 < L < 18000$, used in [4] that indicates the vanishing of the current (velocity) as $L \rightarrow \infty$. The curvature shown in the figure indicates that the velocity will saturate in a nonzero value as $L \rightarrow \infty$. If we adjust the stationary velocity of Fig. 11 as $v(t \rightarrow \infty, L) = A/L^{z-\alpha} + v_\infty$ we obtain for $u = 5$, $z - \alpha = 0.242$ and $v_\infty = 0.0255$. Repeating the procedure for other values of u we obtain the limiting velocities $v_\infty = v(t \rightarrow \infty, L \rightarrow \infty)$ shown in Fig. 12, and the exponents $z - \alpha$ shown in Fig. 13. As we can see $z - \alpha$ decreases drastically as $u \rightarrow \infty$. A fitted curve for the values $z - \alpha = 0.49/(\ln u + 0.42)^{0.12}$ is shown in red in Fig. 13. The limiting behavior when $u \rightarrow \infty$ is distinct from the one at $w = 1/u = 0$. For $1/u = 0$ the model is equivalent to the TASEP, and the boundary condition is important. For the open case, since the particles do not travel after reaching the lattice border, the model is noncritical, while in the periodic case the model is critical and belongs to the KPZ universality class where $z = 3/2$ and $\alpha = 1/2$, therefore $z - \alpha = 1$. In the next section we are going to see how the profiles expected on the KPZ dynamics appear in the short length scale of the RPM with large values of u .

In order to finish our calculation of the critical exponent z we need to calculate the roughness exponent α . This exponent was obtained by considering windows of the profiles $\{h_i\}$ of size ℓ , localized at the center of the lattice (size L). We fit the first cumulant $\kappa_1(\ell, L) = \langle \omega^2(\ell, L) \rangle$ of the roughness (4.4) to the three distinct behaviors: $f_{b>0}(\ell) = a\ell^b + c$, for $b > 0$, $f_{b<0}(\ell) = a\ell^b + c$, for $b < 0$, or $f_{\ln}(\ell) = a \ln \ell + c$. Among these fits the best one is the one where $\rho = 1 - (\text{correl}(\kappa_1, \hat{\kappa}_1))^2$ has the smallest value. The $\text{correl}(\kappa_1, \hat{\kappa}_1)$

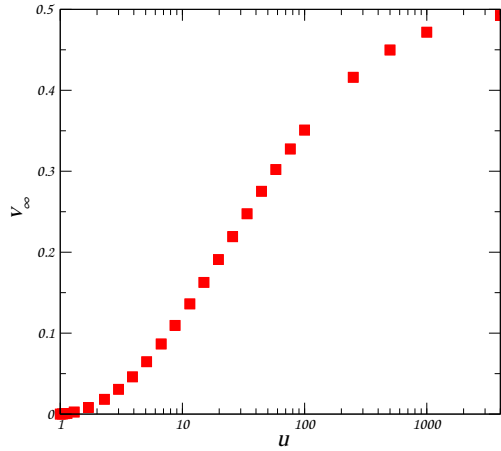


Figure 12: The limiting grow velocity $v_\infty = v(t \rightarrow \infty, L \rightarrow \infty)$ in the stationary state of the periodic RPM, as a function of the parameter u . The results were obtained by averaging 10,048 Monte Carlo samples.

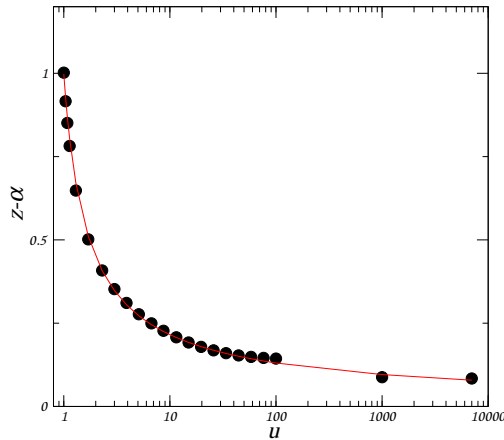


Figure 13: The exponent $z - \alpha$, as a function of u , for the RPM with periodic boundaries (see Eq. (4.5)). The values were obtained by fitting the stationary grow velocity $v(t \rightarrow \infty, L) = AL^{z-\alpha} + v_\infty$. The red line is the fitted curve $g(u) = 0.49/(\ln u + 0.42)^{0.82}$. The maximum error is 9%, and the number of Monte Carlo samples for each lattice size is 10,048. The lattice sizes are $2^6 \leq L \leq 2^{14}$ for all the values of u , except $u = 1000$ and $u = 7000$ where $2^6 \leq L \leq 2^{19}$.

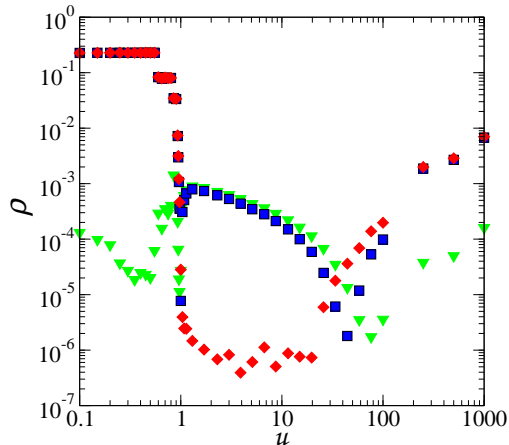


Figure 14: The estimator $\rho = 1 - (\text{correl}(\kappa_1, \hat{\kappa}_1))^2$, as a function of the parameter u , for the fittings of the square of the rugosity $\langle \omega^2 \rangle$ (see Eq. 4.4) of the RPM with periodic boundaries in the stationary regime. The best fittings are the ones with smaller values of ρ . The point in red, green, and blue are the ones where the adjusted behavior, for the windows of size ℓ are $f_{b>0} = a\ell^b + c$ (with $b > 0$), $f_{b<0} = a\ell^b + c$ (with $b < 0$) and $f_{\ln} = \ln \ell + c$, respectively (see also the text).

is the correlation among the original data of κ_1 and the fitted ones. In Fig. 14 we show the values of ρ for the model with periodic and free boundary conditions. The results were obtained for lattice sizes $2^{10} \leq L \leq 2^{14}$ and for the values of $1 \leq u \leq 1000$. We see from these curves that $b < 0$ for $u < 1$ and $u \gtrsim 40$ (green triangles) and $b > 0$ for $1 < u \lesssim 40$ (red squares). We also observe that the logarithmic fittings (blue squares) are reasonable only at $u = 1$ and $u \sim 40$. Using these fits we obtain the values of 2α shown in Fig. 15 (black curve). We also include in Fig. 15 the values of 2α (red curve) obtained for $0.1 < u < 100$ when the RPM is defined in a lattice with free ends. We see an agreement of the estimated values by imposing the two distinct boundary conditions.

These results indicate that for $u > 1$ the RPM has two distinct phases. The transition at $u = u_0 = 1$ can be seen as a roughening transition. For $u < u_c \approx 40$ we have a rough phase with $\alpha > 0$, while for $u > u_c \approx 40$ the surface is not rough ($\alpha < 0$). The values of α in the rough phase are small and vary continuously with u . Since for $1 < u < u_c$ the obtained values of α are small, we should convince ourselves that this variation is not just a finite-size effect, and α could be constant in the whole phase. However performing the evaluation of α by selecting windows of the profiles on distinct ways we obtain almost the same results presented in Fig. 15, indicating that in this rough phase α varies continuously. In order to better understand the nature of the two critical phases we are going to calculate, in the next section, the structure function of the height profiles in both phases.

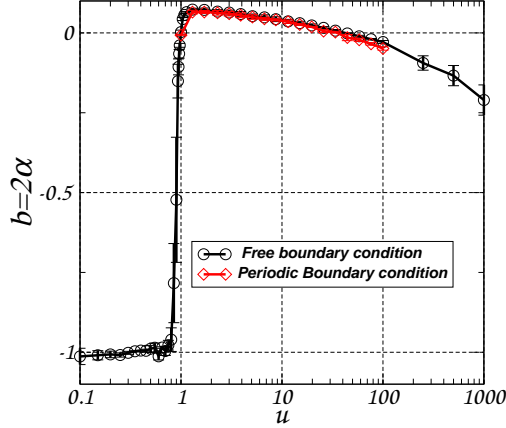


Figure 15: The exponent $b = 2\alpha$ as a function of u . For positive values α is the roughness critical exponent. They are obtained by choosing, in the height profiles, windows of size ℓ and fitting their average to the function $\langle \omega^2(l, L) \rangle = a\ell^b + c$. The curve in black (red) is for periodic (open) boundary conditions, and $\ell = L$ ($1 \ll \ell \ll L$).

5 The structure functions of the height profiles for $u > 1$

The results of the last section indicate that the RPM has, for $u > 1$, two distinct phases. For $1 < u < u_c \approx 40$ the surface profiles are rough with roughness exponent $\alpha > 0$, while for $u > u_c$ the exponent $\alpha < 0$. In this section we calculate the structure functions of the height profiles.

The structure function (2.6) in the stationary regime has the leading behavior, for small values of k or large values of $\lambda = 2\pi/k$: [15]

$$S(k, t \rightarrow \infty) = S(k) \sim k^{-(1+2\alpha)}, \quad (5.1)$$

that depends on the roughness exponent α .

Let us calculate initially the expected behavior of $S(k)$ at the limiting cases $1/u = 0$ and $u = 1$. At $1/u = 0$ the RPM with periodic boundaries recovers the critical TASEP, or equivalently the single step growth model [7, 16]. The height-height correlation function in the stationary state ($t \rightarrow \infty$) of this last model, for heights at position i and j , has the general behavior

$$\langle (h_j - h_i)^2 \rangle - [\langle h_j \rangle - \langle h_i \rangle]^2 = \frac{D}{2\nu}(j - i)^{2\alpha}, \quad 2\alpha = 1, \quad (5.2)$$

where $h_i = h(i, t \rightarrow \infty)$ and $1 \ll j - i \ll L$. In the mapping with the RPM we should take $D = 2$ and $\nu = 1$. Then from (5.1) we obtain, at $1/u = 0$,

$$S(k) \sim \frac{1}{k^2}, \quad (5.3)$$

for large values of $\lambda = 2\pi/k$.

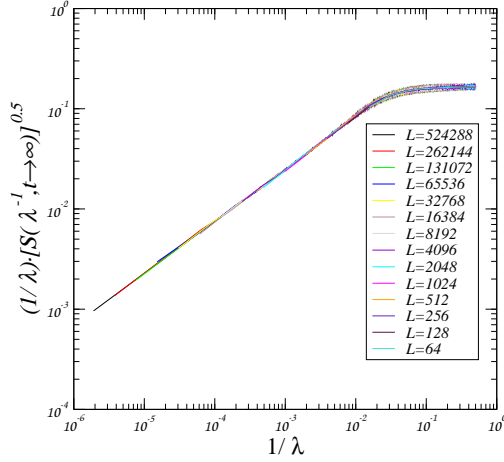


Figure 16: The structure function $S(1/\lambda, t \rightarrow \infty)$, as a function of $1/\lambda$ for the height profiles of the RPM on its stationary regime. The parameter $u = 100$ and the several lattices are shown in the figure. It was considered 14 samples in the Monte Carlos simulation, for each lattice size.

In Fig. 16 we show the stationary structure function $S(1/\lambda)$ of the RPM at stationary time for $u = 100$ and several lattice sizes. We clearly see a crossover region at short length scales $\lambda = 2\pi/k \lesssim 70$. At these short scales $k^2 S(k)$ is constant and the profiles are similar as the ones of the single step height model, or the TASEP, where the roughness exponent is $\alpha = 1/2$. It is interesting to notice that the crossover regions is almost lattice size insensitive.

The other interesting limit of the RPM is the conformal invariant point $u = 1$. At this point by exploring the underlying conformal symmetry of the model it was obtained in [14], that at the stationary time

$$\langle h^2 \rangle - \langle h \rangle^2 = \frac{1}{L} \sum_k S(k) \sim \frac{2\sqrt{3}\pi - 9}{\pi^2} \ln L, \quad (5.4)$$

where $h = h(L, t \rightarrow \infty)$ is the height of a configuration given in (2.4).

Using (5.1) and (5.4) we obtain that $\alpha = 0$ and

$$S(k) \sim \frac{2\sqrt{3}\pi - 9}{\pi} \left(\frac{1}{k}\right). \quad (5.5)$$

In section 3 it was shown in Fig. 7, that for $u < 1$ there exists a crossover region $\lambda < \lambda_c$, that although the system is noncritical it behaves as in (5.5).

In Fig. 17 we show $S(k)$ for a fixed large lattice size $L = 524,288$ and several values of $u > 1$. We clearly see in this figure that even for $u \approx 25$ there exists the crossover region $\lambda < \lambda_c$ where the model exhibits the KPZ behavior ($\alpha = 1/2$). This crossover length $\lambda_c(u)$ increases with u , being infinite at $1/u = 0$. The figure show us that no matter how large is the system the crossover length $\lambda_c(u)$ is finite, and for sufficiently large scales ($\lambda \gg \lambda_c(u)$), the model has a distinct u -dependent behavior. This crossover region, with the KPZ behavior,

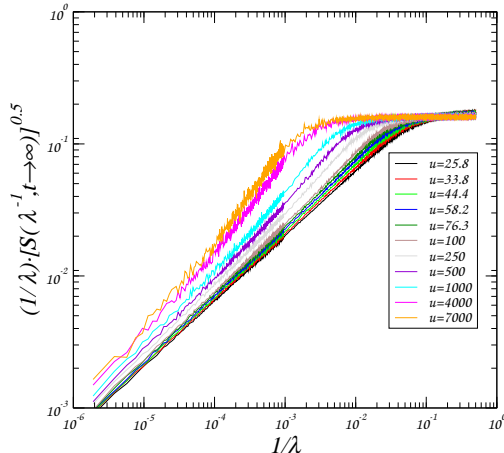


Figure 17: The structure function $S(1/\lambda, t \rightarrow \infty)$ of the height profiles of the RPM with several values of parameter u . The lattice size is $L = 524,288$ and periodic boundary conditions were used.

explains the difficulty in measuring the roughness exponent α directly in the real space, for large values of u . As we increase u we need to consider also larger lattices in order to obtain reasonable estimates for α . However, in the reciprocal space we can separate the behavior at large scales from the small ones. Considering only the large scales we obtain a good estimate for α . To illustrate the sensibility of the structure function, even for small values of α , we show them in Fig. 18, for the lattice size $L = 524,288$ and for $u = 1, 1.3$ and $u = 100$. We clearly see that the large scales gives $\alpha = 0$, $\alpha > 0$ and $\alpha < 0$, respectively.

For small values of k , from (5.1), we estimate the exponent α for several values of $u \geq 1$ ($1/u = w < 1$). The estimates obtained for the lattice size $L = 2^{19} = 524,288$ are the black dots in Fig. 19 (red curve). For the sake of comparison we also show in this figure the estimated values of α obtained in Fig. 15. The results obtained from the structure function calculations, that we believe are more precise, as compared with the one obtained in last section, give us the fitted curve (continuous black curve in Fig. 15):

$$2\alpha = \frac{b \frac{1}{u^c}}{b + a \ln u} - 1, \quad (5.6)$$

with $a = 0.0188(1)$, $b = 0.9290(3)$ and $c = 12.2(4)$. These results confirm the ones obtained previously in the last section and indicate that the system is in a rough phase ($\alpha \geq 0$) for $1 \leq u \leq u_c \simeq 40$ and for $u > u_c$ the system is in phase that at large scales is flat ($\alpha > 0$).

6 Summary and conclusions

In this paper we present an extensive study of the raise and peel model (RPM) with open and periodic boundary conditions. The dynamical processes defining the time evolution of the RPM are local adsorptions and nonlocal desorptions (avalanches). The relevant parameter of the model is the ratio u ($0 \leq u$) among the adsorption and desorption rates. At $u = 1$

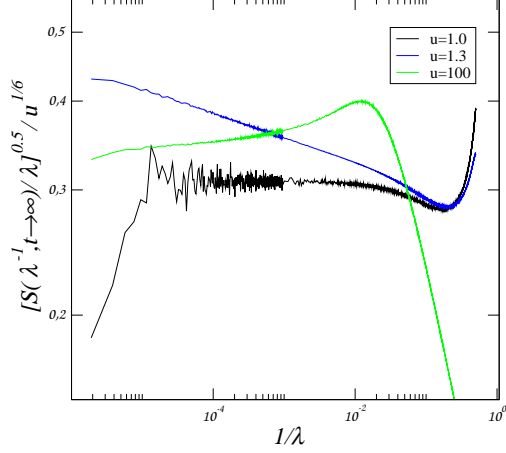


Figure 18: The structure function $S(1/\lambda, t \rightarrow \infty)$ of the height profiles of the RPM with parameters $u = 1, 1.3$ and 100 . The lattice size is $L = 524, 288$ and periodic boundary conditions were used. Notice that a multiplicative factor $u^{1/6}$ was inserted in the vertical axis in order to better visualize the three curves.

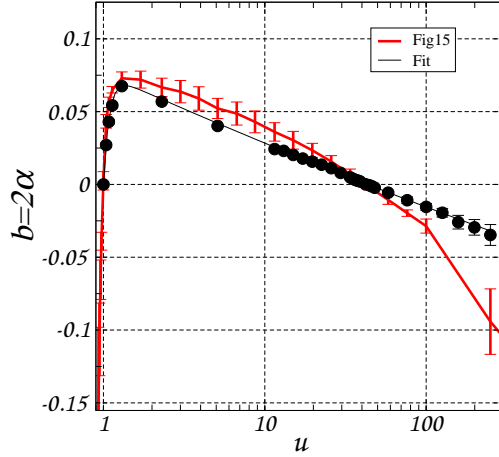


Figure 19: The estimated values of the exponent $b = 2\alpha$, as a function of u . The black dots are the results obtained from the structure function behavior at large scales and the red curve are the ones shown in Fig. 15, obtained by adjusting the behavior of the square of the rugosity in windows of several sizes. The continuum black curve is a fitting one (see the text).

the RPM give us the first example of a conformally invariant stochastic model. Previous studies of the RPM [1, 2] indicate that for $u < u_0$ the model is massive (noncritical) while for $u > u_0$ the model is in a critical phase. The critical point u_0 is not simple to evaluate, although previous results indicate that $u_0 = 1$. In this paper we obtain a precise evaluation of $u_0 = 1.000(1)$. This was done by calculating the structure function of the height profiles in the reciprocal space. Our results explains the difficulty in evaluating u_0 by direct measures of observables. There exists for $1 > u \gtrsim 0.4$, where the model is clearly massive, a crossover region at short scales $\lambda < \lambda_c(u)$, where the model has an effective behavior similar as the one at the critical conformal invariant point $u = 1$. This crossover length $\lambda_c(u)$ grows and diverges at $u = u_0 = 1$. If we do not consider only the large scales $\lambda > \lambda_c(u)$, as we do in direct measurements of observables, when u is close to $u_0 = 1$ the crossover behavior dominates, preventing us to obtain the large-distance physics of the model.

Since at $u_0 = 1$ the roughness exponent $\alpha = 0$ is known exactly [14], we establish that the RPM has a roughness transition at the conformal invariant point $u = u_0 = 1$.

For $u > 1$ previous results [2, 4] indicate that the RPM is in a critical phase, with self-organized criticality having a dynamical critical exponent $z(u)$ that decreases continuously with the parameter u . On the other hand, as noticed in [6], in the limit $1/u = 0$ the RPM is exactly mapped into the TASEP, a model with quite distinct properties, if the boundary conditions are taken to be open (free) or closed (periodic). For open boundary conditions the model is massive and for the periodic ones the model is critical and belongs to the KPZ critical universality with $z = 3/2$ and $\alpha = 1/2$. The estimated value $z(u \rightarrow \infty) = 0$ of the dynamical critical exponent of the RPM was obtained by applying open boundary conditions [2]. The above mapping of the RPM with the TASEP clearly rises the question if the physical behavior of the RPM, for large values of u , is also boundary condition dependent as happens at $1/u = 0$. Our results indicate that this is not the case. Although $z(u) \rightarrow 0$ as $u \rightarrow \infty$, with a roughness exponent $\alpha < 0$, at the limit $1/u = 0$ the model has the KPZ exponents $z = 3/2$ and $\alpha = 1/2$. This is an effect of the non locality of the model. As long $1/u \neq 0$ the nonlocal processes of the RPM produce the same long-distance behavior in both boundaries. Our calculations of the dynamical critical exponents $z(u)$ for the RPM with $u > 1$ were done initially by exploring the L -dependence of the mass gaps of the Hamiltonian on small lattice sizes $L \leq 30$. Better estimates of $z(u)$ could be obtained, in principle, from the time evolution of observables. Our results show, however, that for quite large times the time dependence is distinct for different initial conditions. This effect is known as critical initial slip [10] and forbid us to get reliable results since $z(u)$ is small for large values of u . In order to avoid this large memory effect we need to relate $z(u)$ with a quantity that can be measured directly in the stationary state ($t \rightarrow \infty$). We found this quantity in the periodic case. For this boundary condition the average height grows with time and the we relate the growth's velocity of the surface with the difference of the critical exponents $z(u) - \alpha(u)$.

We evaluate the roughness exponent $\alpha(u)$ directly from the roughness of the surface and surprisingly we found that the region $u > 1$ is not a single phase but is composed by two critical phases. For $u < u_c \approx 40$ the model is rough with a positive exponent $\alpha(u) > 0$, while for $u > u_c$ the model is not rough having $\alpha(u) < 0$.

In order to better understand the critical phases for $u > 1$ we evaluate the structure functions of the height profiles in the reciprocal space. These calculations show us that as

long $u \geq 1$ the KPZ behavior is present in the RPM at short length scales. The crossover region, where the model has a KPZ behavior, grows with the parameter u , becoming infinite only at $1/u = 0$, where indeed the model is equivalent to the TASEP. Although the estimated values of the roughness exponents $\alpha \lesssim 0.02$ are small the behavior of the structure function at large scales (k small) clearly indicates that the phase $1 \leq u \leq u_x \approx 40$ is rough while the phase $u > u_c$ is flat for the large length scales.

7 Acknowledgments

It is a great pleasure to thank Vladimir Rittenberg for numerous and stimulating discussions throughout the course of this work, and also for a careful reading of the manuscript. This work was supported in part by the Brazilian funding agencies: FAPESP, CNPq and CAPES.

References

- [1] De Gier J, Nienhuis B, Pearce P A and Rittenberg V 2004 *J. Stat. Mech.* **114** 1–35
- [2] Alcaraz F C, Levine E and Rittenberg V 2006 *J. Stat. Mech.* **P08003**
- [3] Alcaraz F C and Rittenberg V 2007 *J. Stat. Mech.* **P07009**
Alcaraz F C, Pyatov P and Rittenberg V 2008 *J. Stat. Mech.* **P01006**
- [4] Alcaraz F C and Rittenberg V 2013 *J. Stat. Mech.* **P09010**
- [5] Derrida B, Domany E and Mukamel D, 1992 *J. Stat. Phys.* **69** 667
Derrida B, Evans M R, Hakim V and Pasquier V, 1993 *J. Phys. A* **26** 1493
- [6] Jara D A C and Alcaraz F C 2017 *J. Stat. Mech.* **043205**
- [7] Derrida B, Evans M and Mukamel D 1993 *J. Phys. A: Math. Gen.* **26** 4911
- [8] Derrida B and Mallick K 1997 *J. Phys. A: Math. Gen.* **30** 1031
- [9] Kardar M, Parisi G and Zhang Y-C 1986 *Phys. Rev. Lett.* **56** 889
Halpin-Healy T and Zhang Y-C, 1995 *Phys. Rep.* **254** 215
- [10] Henkel M, Hinrichsen H, Lübeck S and Pleimling M 2008 *Non-equilibrium phase transitions* vol 1 (Springer)
Ódor G 2008 *Universality in nonequilibrium lattice systems* (World Scientific)
Grassberger P and Torre A D L 1979 *Ann. Phys.* **122** 373
Jansen H, Schaub B and Schmittmann B 1989 *Zeitschrift für Physik B* **73** 539
- [11] Barabási A L and Stanley H E 1995 *Fractal concepts in surface growth* (Cambridge university press)
Reis F A 2001 *Phys. Rev. E* **63** p056116
- [12] Razumov A V and Stroganov Yu G 2001 *J. Phys. A: Math. Gen.* **34** 3185

- [13] Kertész J and Wolf D E 1989 *Phys. Rev. Lett.* **62** 2571
- [14] Alcaraz F C and Rittenberg V 2015 *J. Stat. Mech.* **P11012**
- [15] Lie D and Plischke M 1988) *Phys. Rev. B* **38** 4781
- [16] Huse D A, Henley C L and Fischer D S 1985 *Phys. Rev. Lett.* **55** 2924